The quantum nature of the superconducting hydrogen sulfide at finite temperatures

Ying Yuan,[1] Yexin Feng,[2] Lifeng Bian,[3] Dong-Bo Zhang,[4] and Xin-Zheng Li[1, 5, *]

[1]*School of Physics, Peking University, Beijing 100871, P. R. China*
[2]*School of Physics and Electronics, Hunan University, Changsha 410082, P. R. China*
[3]*Key Laboratory of Nanodevices and Applications,*
Suzhou Institute of Nano-Tech and Nano-Bionics,
Chinese Academy of Sciences, Suzhou 215123, Jiangsu, P. R. China
[4]*Beijing Computational Science Research Center, Beijing 100193, P. R. China*
[5]*Collaborative Innovation Center of Quantum Matter, Beijing 100871, P. R. China*
(Dated: September 29, 2018)

H_3S is believed to the most possible high-temperature superconducting (T_c) phase of hydrogen sulfide at $\sim$200 GPa. It's isotope substitution of hydrogen (H) by deuterium (D), however, shows an anomalous T_c decrease of $\sim$100 K at 140 to 160 GPa, much larger than the Bardeen-Cooper-Schrieffer theory prediction. Using *ab initio* path-integral molecular dynamics (PIMD), we show that the nuclear quantum effects (NQEs) influence the structures of H_3S and D_3S differently at finite temperatures and the interval when H_3S possesses the symmetric high T_c structure while D_3S does not is in agreement with, though their absolute values are lower than experiments. This is consistent with an earlier theoretical study using the stochastic self-consistent harmonic approximation method in descriptions of the nuclei at 0 K. The remaining discrepancy can be substantially improved when the electronic structures are calculated using a hybrid function. Our study presents a simple picture to interpret the isotope dependent of T_c and emphasizes the quantum nature in the high-pressure hydrogen sulfide system.

I. INTRODUCTION

A superconductor is a material which exhibits zero electric resistance under a transition temperature (T), *i.e.* T_c. Ever since its discovery in mercury in 1911 [1], understanding the mechanism of this behavior and seeking for high-T_c superconductor have ranked among the biggest challenges in physics. Stimulated by the isotope-dependence of T_c observed in a wide range of superconductors, Bardeen, Cooper, and Schrieffer (BCS) proposed the microscopic picture of electron-phonon coupling in their seminal work in the 1950s [2, 3], which explains the mechanism of most superconductors discovered by then. In 1986, a record-high 133 K T_c was found in copper oxide at ambient pressure [4], followed by a 164 K T_c in a similar system under pressure [5], and the discovery of a series of alike superconductors [6–8]. At present, the superconducting nature for most of these later found superconductors remains unclear. Consequently, it is customary to call the superconductors whose superconducting behaviors can be explained by BCS theory as the conventional ones.

Since BCS theory gives a clear guide to design high T_c conventional superconductors, (*i.e.* a high density of states close to the Fermi level, a favorable combination of high-frequency phonons, and a strong electron-phonon coupling), metallic hydrogen and hydrogen-rich compounds were naturally chosen as the target [9, 10]. Accordingly, a series of theoretical studies on hydrogen and hydrides had been carried out (SiH_4[10], SnH_4[10], GeH_3[11], GeH_4[12], KH_6[13], CaH_6[14], etc). The crystal structure searching methods had played a crucial role [14–16]. For example, a high T_c value of 98 to 107 K

was predicted in $SiH_4(H_2)_2$ at 250 GPa (using a Coulomb parameter $\mu^* = 0.1 - 0.13$, hereinafter, see references for the details) [17]. In $GeH_4(H_2)_2$, a T_c value of 76 to 90 K was predicted at 250 GPa [18]. In MH_3 (M= Ga, Ge, Si) hydrides, T_c values scattering from 76 K to 153 K were reported [11, 19, 20]. In CaH_6, a record-high T_c of 220 to 235 K was reported at 150 GPa [14]. In spite of these exciting theoretical results, it is fair to say that the system which has attracted most attention resides on the recent discovered hydrogen sulfides [21–27], especially after its experimental observation of a 203 K T_c based on direct transport measurement [28].

Now, a consensus has been reached that the stable compound of hydrogen and sulfur at ambient pressure, *i.e.* H_2S, becomes unstable at high pressures. The superconducting behavior at 200 GPa is very likely due to its decomposition to H_3S [22, 23, 25–27]. Comparisons of the *ab initio* static enthalpy based on density-functional theory (DFT) calculations (using the PBE functional) have shown that the stoichiometry decomposition of H_2S to H_3S and S happens at 43 GPa, and H_3S remains stable at least up to 300 GPa [23]. Within this stability range of H_3S, an orthorhombic $Cccm$ structure dominates the group state between 43 and 112 GPa. Then, the rhombohedral $R3m$ phase takes over and it remains most stable till 175 GPa. After 175 GPa, the cubic $Im\bar{3}m$ structure becomes the most stable phase. Calculations of the T_c based on BCS theory using this $Im\bar{3}m$ structure of H_3S (D_3S), in the mean time, show that this value can be as high as $\sim$200 K ($\sim$160 K). In experiments, the T_c of H_3S (D_3S) was measured to be $\sim$190 K ($\sim$150 K) at 170 GPa [28]. This agreement provides an excellent rationalization of the high T_c phase with the $Im\bar{3}m$ structure.

We note, however, that an isotope-dependence for the transition pressure to high T_c exists in experiment, *i.e.* H_3S enters into the high T_c region by $\sim$20 GPa earlier than D_3S [28]. Considering the fact that these theoretical studies are mostly based on static geometry optimizations, the isotope-dependence of the experimental observation, especially the intrinsic anharmonic effects and the nuclear quantum effects (NQEs), are rarely discussed.

Recently, using the stochastic self-consistent harmonic approximation (SSCHA) method for the treatment of nuclear motion [29, 30], Errea *et al.* showed that the phonon spectra of H_3S are highly anharmonic and the anharmonic correction to the phonon spectra has a non-negligible influence on the values of T_c [24]. When taking into account of their contribution to the free-energy as the hydrogen (H) moves along hydrogen-bond, they further demonstrated that the hydrogen-bond symmetrization in superconducting H_3S has a strong quantum nature [31]. Upon replacing H by its isotope deuterium (D), which has only one extra neutron and therefore possesses less NQEs, the pressure with which the system transforms to the symmetric $Im\bar{3}m$ structure increases by 12 GPa at 0 K. Considering the fact that T_c of the ansymmetric rhombohedral $R3m$ phase has a much lower T_c than the cubic $Im\bar{3}m$ phase, this quantum symmetrization of the hydrogen position along the S-H$\cdots$S axis presents a clear picture for the isotope-dependence of the transition pressure with which T_c suddenly increases in H_3S and D_3S. Their absolute values are still lower than the experimental observation by $\sim$50 GPa. We note that this idea of quantum symmetrization was originally proposed in studies of high-pressure H_2O [32, 33], and *ab initio* path-integral molecular dynamics (PIMD) simulations have played an important role in their rationalization [34]. Confirmation of this picture and providing more physical insight to this phase transition by going to finite Ts, using methods like *ab initio* PIMD, are necessary. In addition to this, the PBE functional was used in descriptions of the electronic structure in Ref. 31[35]. It is well-known that these generalized gradient approximations (GGAs) to the exchange-correlation (XC) potential often underestimate the proton transfer energy barrier in hydrogen-bonded systems [36]. A systematic study of the other exchange-correlation functional's influence on this symmetrization pressure is highly desired.

Based on this consideration, we report in this manuscript a theoretical study on the H_3S symmetrization, using *ab initio* PIMD for the description of the NQEs at finite Ts. The accuracy of standard GGA functional was analyzed by comparing the potential energy surface (PES) of the hydrogen along the S-H$\cdots$S axis with a hybrid functional. At 90 and 160 K, our simulations show that NQEs influence the structures of H_3S and D_3S differently and the interval when H_3S possesses the symmetric high T_c structure while D_3S does not is in agreement with, though their absolute values are lower

than experiments. This is consistent with a earlier theoretical study in Ref. 31 where the SSCHA method was used at 0 K. The remaining discrepancy with experiments can be substantially decreased when the electronic structures are described beyond PBE. Our study presents a simple picture to interpret the isotope-dependent of T_c, rationalizes the remaining discrepancy with experimental using higher-level structures, and emphasizes the quantum nature of the high-pressure hydrogen sulfide system.

The paper is organized as follows. The computation details are given in Sec. II. In Sec. III, we presents our results on the quantum nature of the S-H$\cdots$S axis symmetrization, as well as an analysis of the influence of functionals. We draw our conclusions in Sec IV.

II. COMPUTATIONAL DETAILS

Our simulations were preformed using the Vienna *ab initio* Simulation Package (VASP) code [37, 38], along with our own implementation of the PIMD method [39–44]. DFT was used to describe the electronic structure "on-the-fly" as the path of the nuclei propagates. Projector augmented wave (PAW) potentials along with a 700 eV energy cutoff were employed for the expansion of the electronic wave functions [45, 46]. The Perdew-Burke-Ernzerhof (PBE) functional was used to describe the electronic exchange-correlation interaction [35]. With a supercell containing 96 atoms and a Monkhorst-Pack k-point mesh of spacing $2\pi \times 0.04 \text{Å}^{-1}$ to sample the Brillouin zone, we performed *ab initio* PIMD simulations at 90 and 160 K. The Andersen thermostat was chosen to control the temperature of the NVT ensemble [47], in which the atomic velocities were periodically randomized with respect to the Maxwellian distribution every 60 fs.

For the reported results, 16 beads were used. All statistics of the bond length were obtained using the centroid of the path, and we note that using the bond lengths in the individual beads gives the same results. The PBE exchange-correlation functional used in the PIMD simulations suffers from self-interaction errors, which may induce a substantial underestimation of the transition-state energy [36]. We investigate this effect by focusing on the transition barrier and transition distance of the hydrogen atoms as they move along the S-H$\cdots$S axis between their equivalent positions, and comparing the values obtained using the PBE and the hybrid HSE06 functional [48, 49]. In determining these energy barriers, the climbing image nudged elastic band (cNEB) method was used [50], in which all force components that perpendicular to the tangent of the reaction path were reduced to less than 0.01 eV/Å.

III. RESULTS AND DISCUSSIONS

IIIa. Quantum Nature of the Phase-Transition

We start by looking at the structures of the rhombohedral $R3m$ phase and the cubic $Im\bar{3}m$ phase at the static level. Although being rhombohedral, $R3m$ is very close to cubic symmetry. This can be evidenced by looking at the rhombohedral angle of $R3m$, which is 109.5142, 109.5476, and 109.5592, respectively at 140 GPa, 150 GPa, and 160 GPa, in comparison with the value of 109.47° for a perfect bcc lattice. Therefore, we visualize the difference between the structures of these two phases in Fig. 1 a) and b), using a slightly distorted bcc cell of the $R3m$ phase and the conventional bcc cell of the cubic $Im\bar{3}m$ phase. The S atoms stay on a slightly distorted bcc lattice in the $R3m$ phase and the conventional bcc lattice in the $Im\bar{3}m$ phase. The difference between these two lattices is visually indistinguishable. The H atoms, however, show very different behaviors. In the $R3m$ phase, the H atoms stay asymmetrically along the S-H$\cdots$S axis, being closer to one S atom. If we label the covalent bond length S-H as d_1 and the distance between the H atom and its next nearest S atom as d_2, these two distances are unequal. In the $Im\bar{3}m$ phase, however, they are symmetric, with $d_1 = d_2$. Therefore, the main change happened during the phase transition from the $R3m$ phase to the $Im\bar{3}m$ phase, lies on the symmetrization of S-H$\cdots$S, instead of the rhombohedral to cubic lattice evolution. This can be clearly seen in Fig. 1 c) and d), where we show that using a rhombohedral lattice for the symmetric structure ($R\bar{3}m$) or a cubic lattice for $R3m$ (fix$R3m$) has negligible effect on enthalpy differences of these two phases, and by imposing rhombohedral or cubic lattice for $R3m$, the symmetrization happens at very close pressures. In Ref. 31, a cubic cell has been used in discussion of the phase transition in. Here, we adopt a rhombohedral cell in discussions of the classical and quantum nuclear effects at finite Ts. By comparing with their results, one will see that the quantum feature of hydrogen-bond symmetrization is robust with respect to this choice of the simulation cell.

Now we include the nuclear statistical effects at the classical level. This is done by carrying out the *ab initio* molecular dynamics (MD) simulations at 90 K for a supercell of the $R3m$ phase. We define a H transfer coordinate $\delta = d_1 - d_2$. When it is zero, the hydrogen bond is symmetric and the H atom is equally shared by the two S atoms. When it is large in magnitude on both positive and negative sides, the H belongs to one S atom. The results are shown in Fig. 2 a) and b). It is clear that although the hydrogen bond symmetrization happens at $\sim$170 GPa at the static level, this transition pressure is substantially decreased at a finite T upon including the nuclear classical statistical
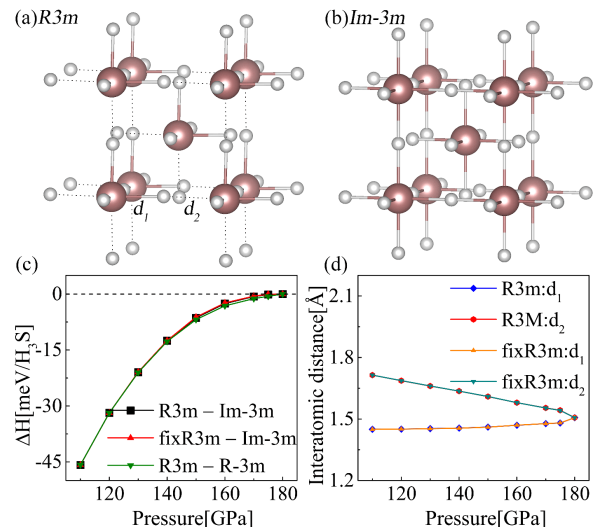

FIG. 1. Static crystal structures of the $R3m$ (panel a) and $Im\bar{3}m$ (panel b) phases. A slightly distorted bcc lattice is used for the $R3m$ phase and the conventional bcc lattice is used for $Im\bar{3}m$. d_1 and d_2 are the distance between the H atom and its two nearest neighboring S atoms. In $R3m$, these two values are not equal. In $Im\bar{3}m$, they are. In c), we compare the enthalpy differences of the $R3m$ and $Im\bar{3}m$ phases by imposing a cubic lattice for $R3m$ (fix$R3m$) or a rhombohedral lattice for the symmetric structure ($R\bar{3}m$). In d), we monitor the evolution of d_1 and d_2 using the cubic and the rhombohedral cells. These two panels show that imposing the rhombohedral symmetry has a negligible influence on the symmetrization of the hydrogen bonds. Summing up these four panels, we would say that the main structural change upon transforming from $R3m$ to $Im\bar{3}m$ lies on symmetrization of the hydrogen bonds.

effects. At 140 GPa, the probability distribution ($P(\delta)$) has two clear peaks at δ equals ± 0.2 Å, indicating that the hydrogen bonds are still asymmetric. At 150 GPa, it has a single peak at $\delta = 0$, a clear indication of hydrogen bond symmetrization. Therefore, the symmetrization of the hydrogen bond happens in between 140 and 150 GPa, when the nuclear classical statistical effects are included at 90 K. This symmetrization is also confirmed by the corresponding free-energy profile calculated using $\Delta F(\delta) = -k_B T \ln P(\delta)$, where the single- and double-valley feature of the profiles tells us where the H atoms want to stay. In comparison with the static results, with classical nuclei, the symmetrization moves toward a lower pressure at a finite T.

Then we include the NQEs for D at the same T. The structure is analyzed in a similar way, using the centroid of the path-integral in Fig. 2 c) and d). At 90 GPa, $P(\delta)$ ($\Delta F(\delta)$) shows a double-peak (double-well) structure, indicating that the hydrogen bonds are still not symmetric. At 100 GPa, however, the single-peak (single-well) structure already appeared, meaning that the hydrogen bond symmetrization happened. Therefore, the transi-
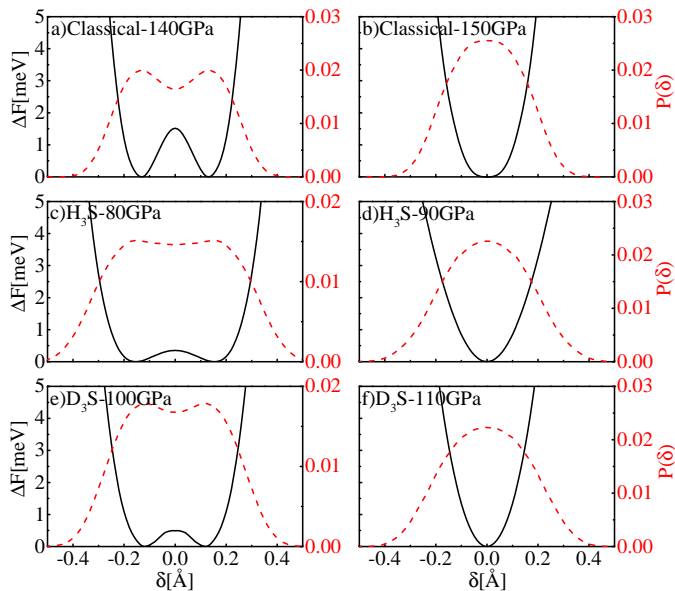
FIG. 2. Symmetrization of the hydrogen bonds. Using the H transfer coordinate (defined as $\delta = d_1 - d_2$), the probability distribution $P(\delta)$ and the free-energy profile $\Delta F(\delta)$ are plotted to the left and right scales based on *ab initio* MD and *ab initio* PIMD simulations at 90 K. Panels a) and b) correspond to results using classical nuclei, where the upper bound for the asymmetric structure and lower bond for the symmetric structure are reported within numerical resolution of 10 GPa. Panels c) and d) correspond to results obtained using quantum nuclei for D_3S. And panels e) and f) correspond to results obtained using quantum nuclei for H_3S.

tion from asymmetrized to symmetrized hydrogen bond happens between 90 and 100 GPa in D_3S. In H_3S, on the other hand, this symmtrization happens between 80 and 90 GPa (Fig. 2 e) and f)).

We note that these values for H_3S and D_3S are lower than the transition pressures of 103 and 115 GPa when quantum nuclei are used at 0 K. To investigate in more detail the T-dependence of this transition pressure, we carried out a separate series of *ab initio* MD and *ab initio* PIMD simulations at 160 K. Using right- and left-solid triangles, we label the upper and lower boundary of asymmetric and symmetric structures in Fig. 3, along with results discussed earlier for the 90 K simulations. The results reported for classical nuclei and quantum nuclei (both D_3S and H_3S) at 0 K in Ref. 31 were also labelled using diamond, solid circle, and open circle respectively. From these figure, it is clear that while being consistent with the isotope-dependence of the symmetrization pressure as reported in Ref. 31, our simulations also show that the symmetrization happens at lower pressures upon increasing T. This is also in agreement with a series of earlier hydrogen bond symmetrization study of ice under pressure [32–34, 51]. Considering the fact that symmetric $Im\bar{3}m$ phase exhibits a much higher T_c than the asymmetric $R3m$ phase when calculations based on

BCS theory is used [22], this presents a clear picture for the isotope-dependence of the transition pressure of H_3S and D_3S to the high T_c phase [28]. In comparison with the results obtained using classical nuclei, the hydrogen bonds in H_3S are strongly quantum in nature.
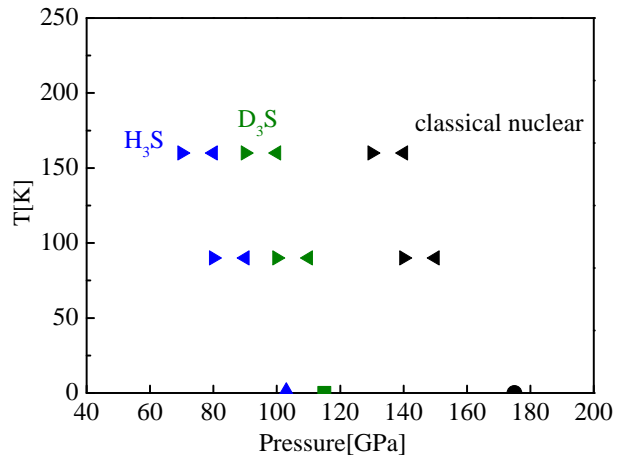

FIG. 3. T-dependence of the hydrogen bond symmetrization using classical nuclei, and quantum nuclei for D_3S and H_3S. The upper (lower) bounds of the asymmetric (symmetric) hydrogen bonds are labelled using left-(right-)oriented triangles respectively. Two series of *ab initio* MD and *ab initio* PIMD simulations are reported. The results from Ref. 31 for classical nuclei and quantum nuclei (D_3S and H_3S) at 0 K were labelled using blue upward triangle, green half square, and black half circle.

IIIb. Deficiency of PBE Functional

In spite of the qualitatively excellent agreement between the theoretical and experimental results, as reported above and in Ref. 31, a large discrepancy still exists. The predicted symmetrization happens at a pressure ∼60 GPa lower than the experimental observation. Considering the fact that the proton-transfer energy barriers and the distance of proton transfer play an important role for such a symmetrization [51], and the PBE functional used here and in Ref. 31 is well-known to underestimate the transition state (TS) energy in description of the chemical reactions [36], it is reasonable to expect that the deficiency of the PBE functional plays a key role on the underestimation of this transition pressure. Based on this consideration, we investigate the functional-dependence of the symmetrization pressure.

For periodic system, the easiest way to check this underestimation of the TS energy, mostly due to the delocalization error [36], is to compare the results obtained from the hybrid-functional calculations with those obtained from the standard local-density approximation (LAD) or generalized-gradient approximation (GGA) calculations. However, considering the fact that the com-
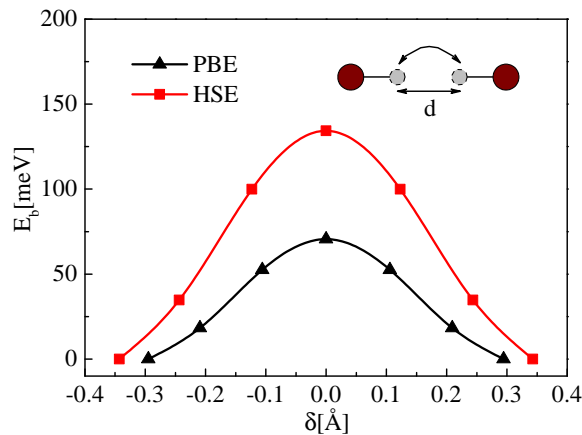
FIG. 4. TS searching based on the cNEB method for the proton transfer process. The red squares are obtained using HSE06. The black triangles are obtained using PBE. Upon including partial exact exchange, the proton transfer barrier and the proton transfer distance increase. This is a clear indication that self-interaction substantially underestimates these quantities, and consequently underestimates the symmetrization pressure.
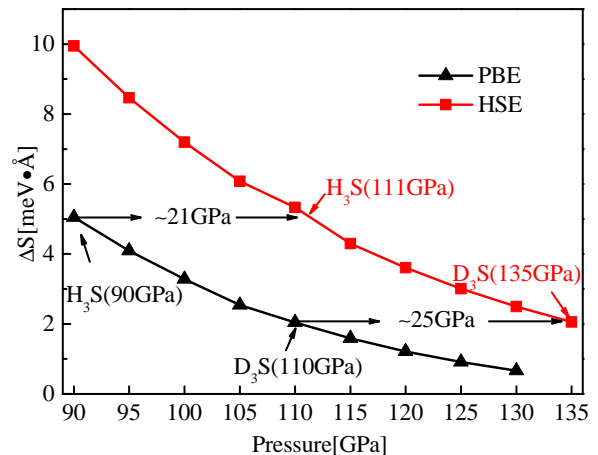

FIG. 5. Estimation of the symmetrization pressure, using $\Delta S = d \times \Delta E$, as the descriptor. The upper horizontal line at $\Delta S \sim 5$ indicates the situation when H_3S symmetrization is confirmed. The upper horizontal line at $\Delta S \sim 2$ indicates the situation when D_3S symmetrization is confirmed. Based on this extrapolation, we estimate that using the HSE function will increase the symmetrization pressure of H_3S (D_3S) by 21 (25) GPa, toward the experimental results.

putational cost of performing a hybrid-functional based PIMD simulation is beyond what we can afford, we carried out such an analysis at the static level. The cNEB method is used to find the TS for the H atom transfer from one S atom to the other. The energy-profiles are shown in Fig. 4 for the simulation at 100 GPa. From this figure, it is clear that the PBE functional has underestimated the proton transfer energy barrier by 50% in comparison with the HSE06 based results. Considering the fact that partial exact-exchanges are included in this hybrid-functional, which helps to cure the artificial electron charge delocalization induced by self-interaction [36], this is a clear indication that PBE has underestimated the proton transfer energy barrier. Consequently, when the *ab initio* PIMD simulations are performed using electronic structures provided by the DFT calculations using PBE functional, a systematic underestimation of the symmetrization pressure occurs. We note that a similar underestimation of the transition pressure also happens in the molecular liquid dissociation to the atomic liquid phase in high-pressure hydrogen, as pointed out in Ref. 40. Upon including more exact-exchange interaction in this HSE-based functional, this underestimation is even more serious. Therefore, we believe that the right answer for proton transfer energy barrier must lie somewhere much higher than the PBE result. A quantitative determination of this value requires more sophisticated electronic structure methods, which is beyond the scope of the present paper.

Finally, despite hybrid-functional based *ab initio* PIMD simulations are beyond the computational cost we can afford, due to the fact that extend of proton delocal-

ization is sensitive to the area below the proton transfer energy profile, an estimation of the symmetrization pressure can be provided. An estimator ΔS is defined as $(d \times \Delta E)/2$ and plotted as a function of pressure in Fig. 5. The definition of d is given in the inset of Fig. 4. At each pressure, this ΔS is obtained by two steps. First, an enthalpy-based geometry optimization is carried out using DFT calculations with PBE and HSE06 functionals. The difference between the two symmetrized structures with the H atom belonging to each S gives us d. Then, ΔE is calculated using the cNEB method, again based on DFT calculations with PBE and HSE06 functionals. The results are shown in Fig. 5. From Fig. 4, we know that the difference between the values of d is small and the difference between values of ΔE is large between DFT calculations with the PBE and the HSE06 functionals. Consequently, at each pressure, the value ΔS is much larger in the HSE06-based DFT calculations compared with the PBE-based DFT calculations. The horizontal dashed line indicates the value of ΔS at which H_3S symmetrizes and the horizontal solid line indicates the value of ΔS at which D_3S symmetrizes. Therefore, an estimation of the symmetrization pressure in the HSE06 functional based PIMD simulations would be 110 GPa for H_3S and 135 GPa for D_3S at 90 K. Compared with the PBE functional based PIMD simulations, these values clearly move toward experimental observation. Again, we note that a better agreement between theory and experiment must require more accurate theoretical methods on the electronic structure level, with NQEs also accurately addressed. This is beyond the scope of most theoretical groups. We focus more on pointing out the deficiency of

the PBE functional, so that further theoretical studies could be aware of in such simulations.

CONCLUSIONS

Based on *ab initio* MD and *ab initio* PIMD simulations, we systematically investigate the influence of nuclear statistical effects on the symmetrization of H_3S and D_3S with classical and quantum nuclei at finite Ts. The accuracy of standard GGA functional was analyzed by comparing the PES of the hydrogen along the S-H$\cdots$S axis with the hybrid ones. Our simulations show that NQEs influence the structures of H_3S and D_3S differently and the interval when H_3S possesses the symmetric high T_c structure while D_3S does not is in agreement with, though their absolute values are lower than the experimental observations. These results at 90 and 160 K are consistent with a earlier theoretical study in Ref. 31 where the SSCHA method was used at 0 K. The remaining discrepancy with experiments can be substantially decreased when the hybrid-functional is used. This study presents a simply picture to interpret the isotope-dependent of T_c. In the meantime, it also rationalizes the remaining discrepancy with experiments by pointing out the deficiency of the PBE functional, and emphasizes the quantum nature of the high-pressure hydrogen sulfide system.

---

* xzli@pku.edu.cn

[1] H. K. Onnes, Commun. Phys. Lab. Univ. Leiden **12**, 120 (1911).

[2] J. Bardeen, L. N. Cooper, and J. R. Schrieffer, Phys. Rev. **106**, 162 (1957).

[3] J. Bardeen, L. N. Cooper, and J. R. Schrieffer, Phys. Rev. **108**, 1175 (1957).

[4] J. G. Bednorz and K. A. Müller, Z. Phys. B **64**, 189 (1986).

[5] L. Gao, Y. Y. Xue, F. Chen, Q. Xiong, R. L. Meng, D. Ramirez, C. W. Chu, J. H. Eggert, and H. K. Mao, Phys. Rev. B **50**, 4260 (1994).

[6] S. N. Putilin, E. V. Antipov, O. Chmaissem, and M. Marezio, Nature **362**, 226 (1993).

[7] A. Schilling, M. Cantoni, J. D. Guo, and H. R. Ott, Nature **363**, 56 (1993).

[8] P. Dai, B. C. Chakoumakos, G. F. Sun, K. W. Wong, Y. Xin, and D. F. Lu, Physica C **243**, 201 (1995).

[9] N. W. Ashcroft, Phy. Rev. Lett. **21**, 1748 (1968).

[10] N. W. Ashcroft, Phy. Rev. Lett. **92**, 187002 (2004).

[11] K. Abe and N. W. Ashcroft, Phys. Rev. B **88**, 174110 (2013).

[12] G. Y. Gao, A. R. Oganov, A. Bergara, M. Martinez-Canales, T. Cui, T. Iitaka, Y. M. Ma, and G. T. Zou, Phys. Rev. Lett. **101**, 107002 (2008).

[13] D. W. Zhou, X. L. Jin, X. Meng, G. Bao, Y. M. Ma, B. B. Liu, and T. Cui, Phys. Rev. B **86**, 014118 (2012).

[14] H. Wang, J. S. Tse, K. Tanaka, T. Iitaka, and Y. M. Ma, Proc. Natl. Acad. Sci. U.S.A. **109**, 6463 (2012).

[15] C. J. Pickard and R. J. Needs, Phys. Rev. Lett. **97**, 045504 (2006).

[16] G. Y. Gao, A. R. Oganov, Z. Li, P. Li, T. Cui, A. Bergara, A. O. Lyakhov, M. Y. M., T. Iitaka, and G. Zou, Proc. Natl. Acad. Sci. U.S.A. **107**, 1317 (2010).

[17] Y. W. Li, G. Y. Gao, Y. Xie, Y. M. Ma, T. Cui, and G. T. Zou, Proc. Natl. Acad. Sci. U.S.A. **107**, 15708 (2010).

[18] G. H. Zhong, C. Zhang, X. J. Chen, Y. L. Li, R. Q. Zhang, and H. Q. Lin, J. Phys. Chem. C **116**, 5225 (2012).

[19] G. Y. Gao, H. Wang, A. Bergara, Y. W. Li, G. T. Liu, and Y. M. Ma, Phys. Rev. B **84**, 064118 (2011).

[20] X. Jin, X. Meng, Z. He, Y. M. Ma, B. B. Liu, T. Cui, G. T. Zou, and H. K. Mao, Proc. Natl. Acad. Sci. U.S.A. **107**, 9969 (2010).

[21] Y. W. Li, J. Hao, H. Y. Liu, Y. L. Li, and Y. M. Ma, J. Chem. Phys. **140**, 174712 (2014).

[22] D. F. Duan, Y. X. Liu, F. B. Tian, D. Li, X. L. Huang, Z. L. Zhao, H. Y. Yu, B. B. Liu, W. J. Tian, and T. Cui, Sci. Rep. **4**, 6968 (2014).

[23] D. F. Duan, X. L. Huang, F. B. Tian, D. Li, H. Y. Yu, Y. X. Liu, Y. B. Ma, B. B. Liu, and T. Cui, Phys. Rev. B **91**, 180502 (2015).

[24] I. Errea, M. Calandra, C. J. Pickard, J. Nelson, R. J. Needs, Y. W. Li, H. Y. Liu, Y. W. Zhang, Y. M. Ma, and F. Mauri, Phys. Rev. Lett. **114**, 157004 (2015).

[25] Y. W. Li, L. Wang, H. Y. Liu, Y. W. Zhang, J. Hao, C. J. Pickard, J. R. Nelson, R. J. Needs, W. T. Li, Y. W. Huang, I. Errea, M. Calandra, F. Mauri, and Y. M. Ma, Phys. Rev. B **93**, 020103 (2016).

[26] N. Bernstein, C. S. Hellberg, M. D. Johannes, I. I. Mazin, and M. J. Mehl, Phys. Rev. B **91**, 060511 (2015).

[27] M. Einaga, M. Sakata, T. Ishikawa, K. Shimizu, M. I. Eremets, A. P. Drozdov, I. A. Troyan, N. Hirao, and Y. Ohishi, Nat. Phys. **x**, xx (2016).

[28] A. P. Drozdov, M. I. Eremets, I. A. Troyan, V. Ksenofontov, and S. I. Shylin, Nature **525**, 73 (2015).

[29] I. Errea, M. Calandra, and F. Mauri, Phys. Rev. Lett. **111**, 177002 (2013).

[30] I. Errea, M. Calandra, and F. Mauri, Phys. Rev. B **89**, 064302 (2014).

[31] I. Errea, M. Calandra, C. J. Pickard, J. R. Nelson, R. J. Needs, Y. W. Li, H. Y. Liu, Y. W. Zhang, Y. M. Ma, and F. Mauri, Nature **532**, 81 (2016).

[32] A. Goncharov, V. V. Struzhkin, M. S. Somayazulu, R. J. Hemley, and H. K. Mao, Science **273**, 218 (1996).

[33] P. Loubeyre, R. LeToullec, E. Wolanin, M. Hanfland, and D. Hausermann, Nature **397**, 503 (1999).

[34] M. Benoit, D. Marx, and M. Parrinello, Nature **392**, 258 (1998).

[35] J. P. Perdew, K. Burke, and M. Ernzerhof, Phys. Rev. Lett. **77**, 3865 (1996).

[36] A. J. Cohen, P. Mori-Sánchez, and W. T. Yang, Chem. Rev. **112**, 289 (2011).

[37] G. Kresse and J. Furthmüller, Comput. Mat. Sci. **6**, 15 (1996).

[38] G. Kresse and J. Furthmüller, Phys. Rev. B **54**, 11169 (1996).

[39] J. Chen, X. Z. Li, Q. F. Zhang, M. I. J. Probert, C. J. Pickard, R. J. Needs, A. Michaelides, and E. G. Wang, Nat. Commun. **4**, 2064 (2013).

[40] J. Chen, X. G. Ren, X. Z. Li, D. Alfe, and E. G. Wang, J. Chem. Phys. **141**, 024501 (2014).

[41] Y. X. Feng, J. Chen, D. Alfe, X. Z. Li, and E. G. Wang, J. Chem. Phys. **142**, 064506 (2015).

[42] J. Guo, J. T. Lu, Y. X. Feng, J. Chen, J. B. Peng, Z. R. Lin, X. Z. Meng, Z. C. Wang, X. Z. Li, E. G. Wang, and Y. Jiang, Science **352**, 321 (2016).

[43] J. Chen, Y. X. Feng, X. Z. Li, and E. G. Wang, Acta Physica Sinica **64**, 183101 (2015).

[44] Y. X. Feng, J. Chen, X. Z. Li, and E. G. Wang, Chinese Physics B **25**, 013104 (2016).

[45] P. E. Blochl, Phys. Rev. B **50**, 17953 (1994).

[46] G. Kresse and D. Joubert, Phys. Rev. B **59**, 1758 (1999).

[47] H. C. Andersen, J. Chem. Phys. **72**, 2384 (1980).

[48] J. Heyd, G. Scuseria, and M. Ernzerhof, J. Chem. Phys. **118**, 8207 (2003).

[49] J. Heyd, G. Scuseria, and M. Ernzerhof, J. Chem. Phys. **124**, 219906 (2006).

[50] G. Henkelman and H. Jónsson, J. Chem. Phys. **113**, 9901 (2000).

[51] X. Z. Li, M. I. J. Probert, A. Alavi, and A. Michaelides, Phys. Rev. Lett. **104**, 066102 (2010).